Design by Advanced Elastic Analysis: An Investigation of Beam-Columns

YUNFEI WANG and RONALD D. ZIEMIAN

ABSTRACT

At the heart of the provisions for assessing structural stability within the AISC *Specification for Structural Steel Buildings* is the direct analysis method. The fundamental concept for this method is that the more behavior is explicitly modeled within the analysis, the simpler it is to define the AISC *Specification* design requirements. In other words, the direct analysis method consists of calculating strength demands and available strengths according to a range of well-defined and fairly detailed analysis requirements. This paper begins with an overview of two logical extensions to AISC's direct analysis method, both of which are now provided in AISC *Specification* Appendix 1, Design by Advanced Analysis. In establishing these approaches, many systems were investigated in previous research, and it was noted that systems with beam-columns subject to minor-axis bending may deserve additional attention. This paper presents a detailed study that investigates such members, as well as members subject to major-axis bending.

Keywords: direct analysis method, design by advanced analysis, design by advanced elastic analysis, beam-column, AISC, steel design.

INTRODUCTION

For the past 60 years, the effective length method (ELM) has been a widely employed stability design method (Ziemian, 2010). By scaling actual unbraced lengths to effective lengths when calculating the available strengths of compression members, the effective length K-factor is assumed to account for most factors known to impact the stability of structural systems, including geometric system imperfections; stiffness reduction due to inelasticity; and, to a much lesser degree, uncertainty in strength and stiffness (AISC, 2016b). In 2005, design by the direct analysis method (DM) first appeared in the AISC *Specification for Structural Steel Buildings* (AISC, 2005), hereafter referred to as the AISC *Specification*. In DM, the available strengths of compression members are based simply on the unbraced length (K = 1), as long as system imperfections (but not member imperfections) and stiffness reduction due to inelasticity are represented in the structural analysis. Since then, many in the structural design profession have moved from employing ELM to DM. As a result, DM was relocated in the 2010 AISC *Specification* (AISC, 2010) from Appendix 7 to Chapter C, while ELM was relocated from Chapter C to Appendix 7.

Both design methods rely on establishing the unbraced lengths of compression members, which in some cases may be difficult, if not impossible, to define. Examples include, but are not limited to, arches, tree columns, and Vierendeel trusses. In response to this predicament, AISC introduced the design by advanced elastic analysis method that appears in the 2016 AISC *Specification* in Appendix 1. In addition to the analysis modeling requirements of DM, the method further requires the direct modeling of member imperfections and, therefore the method is often represented by the acronym DMMI. In applying this approach, engineers can avoid the complexities of defining unbraced lengths, thereby being permitted to compute the nominal available strengths of compression members as their axial cross-sectional strengths. This paper reports on a study to complement previous studies on systems to evaluate the performance of DMMI (Nwe Nwe, 2014; Giesen-Loo, 2016), especially with an eye toward members that are subject to the combination of compression and minor-axis bending (Wang, 2018; Wang and Ziemian, 2019). Using AISC's design by advanced inelastic analysis method, which is based on employing a rigorous geometric and material nonlinear analysis with imperfections (GMNIA), the accuracy of DMMI is assessed and further compared with the more traditional ELM and DM design methods. Additionally, the significances of thermal residual stresses, which are a consequence of uneven cooling of rolled cross sections, and the axis of bending (minor versus major) for W- and HSS shapes are also explored.

The paper begins by providing an overview of AISC's ELM, DM, DMMI, and GMNIA methods, along with details of the analysis method and the interaction equation employed in each. Results of the study are then presented

Yunfei Wang, Gilsanz Murray Steficek, New York, N.Y. Email: phoebe.wang@gmsllp.com

Ronald D. Ziemian, Bucknell University, Civil and Environmental Engineering Department, Lewisburg, Pa. Email: ziemian@bucknell.edu (corresponding)

Paper No. 2019-19

primarily in tabular format, which are followed by discussions of the effects of residual stresses, axis of bending, and design method employed.

OVERVIEW OF DESIGN METHODS

In this study, the ends of simply supported columns of various slenderness ratios are subjected to a wide range of combinations of applied axial force and bending moments that are of equal magnitude and opposite direction (in the absence of axial force, such moments would produce a uniform moment distribution). In all cases, the members are assumed to be fully braced out-of-the-plane of bending. To assess the LRFD strength of beam-columns based on an elastic analysis, the following interaction equations are provided in the AISC *Specification* (from *Specification* Equations H1-1a and H1-1b):

$$\frac{P_u}{\phi P_n}+\frac{8}{9}\left(\frac{M_{ux}}{\phi M_{nx}}+\frac{M_{uy}}{\phi M_{ny}}\right)\leq 1.0 \quad \text{for } P_u/\phi P_n \geq 0.2 \tag{1a}$$

$$\frac{P_u}{2\phi P_n}+\left(\frac{M_{ux}}{\phi M_{nx}}+\frac{M_{uy}}{\phi M_{ny}}\right)\leq 1.0 \quad \text{for } P_u/\phi P_n < 0.2 \tag{1b}$$

where ϕ = 0.90, P_u is the required axial strength, M_u is the required flexural strength, P_n is the nominal available axial strength, and M_n is the nominal available flexural strength about either the major x- or minor y-axis. The analysis for the required axial strength, P_u, and flexural strength, M_u, should consider second-order (geometric nonlinear) effects.

The following design methods, including ELM, DM, and DMMI, employ Equations 1a and 1b with terms defined by that specific method. In all cases, the controlling combinations of axial force and bending moment are determined for each of these elastic design methods by iteratively solving for the maximum value of M_u for a given value of P_u that will satisfy Equation 1. For reference, Figure 1 shows the deflected shape of the beam-column. Equilibrium on the deformed shape is given by:

$$M_u(x,P)+Pv(x)+M=0 \tag{2}$$

After substituting the moment-curvature relationship, $M_u(x,P)=EId^2v/dx^2$, Equation 2 becomes the governing differential equation:

$$EI\frac{d^2v}{dx^2}+Pv(x)=-M \tag{3}$$

where $v(x)$ is the total lateral deflection as a function of span length location x and equals the sum of an assumed geometric imperfection $v_0(x)=\delta_0 \sin\frac{\pi x}{L}$ and deflection $v_{PM}(x)$ due to the applied combination of P and M.

Effective Length Method (ELM)

In computing the nominal axial strength, P_n, from the AISC column curve, the effective length factor of a simply supported beam-column is K = 1. In determining the required flexural strength, M_u, equilibrium equations are

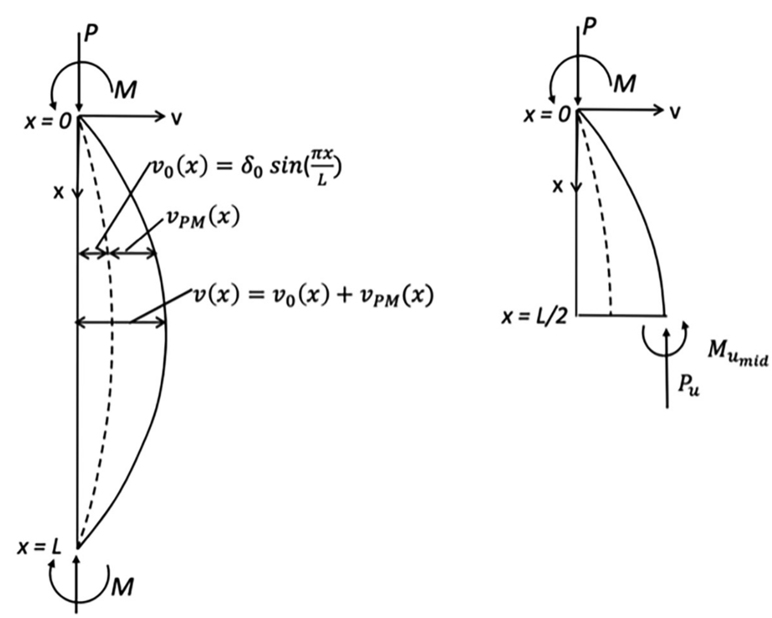

(a) Deflection diagram *(b) Free-body diagram at mid-height*

Fig. 1. Deflected shape of beam-column with second-order effects due to applied loading and geometric imperfection.

defined on the deflected shape to account for second-order effects. For a structural analysis associated with ELM, the beam-column is assumed geometrically straight, $v_0(x) = 0$, prior to any applied loading (the AISC column curve accounts for member out-of-straightness). As a result, the P-δ effect in this method need only account for the interaction between the applied axial load and bending moments and, thereby, is not influenced by the presence of an initial member imperfection.

In establishing the design adequacy of this member, the required moment, $M_u(x,P)$, is a maximum at midspan because $v_{PM}(x)$ takes on a maximum value when $x = L/2$. Thus, the interaction equation only needs to be checked at midspan, where the required strengths (terms in the numerators of Equation 1) are at a maximum. For an elastic analysis of a simply supported, originally perfectly straight, and prismatic member, the required flexural strength, M_u, at midspan, which includes moment amplification due to second-order effects, can be calculated as a function of the applied force P and moment M by the following "exact" equation (McGuire et al., 2000):

$$\left|M_{u_{mid}}\right| = \frac{M}{\cos\left(\frac{\pi}{2}\sqrt{\frac{P}{P_e}}\right)} \tag{4}$$

where P_e is the Euler buckling strength of the beam-column, and noting that shear deformation is neglected.

With $P_u = P$ at midspan, substitution of these terms for P_u and $M_u = \left|M_{u_{mid}}\right|$ in Equation 1a results in an interaction equation for ELM defined by:

$$\frac{P}{\phi P_n} + \frac{8}{9}\left[\frac{\dfrac{M}{\cos\left(\frac{\pi}{2}\sqrt{\frac{P}{P_e}}\right)}}{\phi M_n}\right] \le 1.0 \tag{5}$$

in which, specific to ELM,

$$P_n = F_{cr} A_g$$

$$P_e = \frac{\pi^2 EI}{L^2}$$

$$M_n = F_y Z$$

where F_{cr} is the critical buckling stress as defined by the AISC column curve, with $K = 1$ for the simply supported end conditions being investigated in this study; A_g is the gross area of the cross-section; E is the elastic modulus of the material; I is the moment of inertia; L is the unsupported length of the beam-column; F_y is the material yield stress; and Z is the plastic section modulus. In computing M_n, it is important to note that only members with compact sections are investigated, and any members subject to major-axis bending are assumed fully braced out-of-plane.

Direct Analysis Method (DM)

Although DM permits the use of the unbraced length ($K = 1$), this provides no advantage over ELM for the specific end support conditions of the single beam-column investigated in this study. In fact, DM is somewhat penalized in this case by its required use of a stiffness reduction factor within the structural analysis. Although the equilibrium analysis is of the same form as that given for ELM, the Euler buckling strength, P_e, used in the analysis of the member is modified to represent the inelastic buckling strength of the member. As a result, the interaction equation (Equation 1a) for DM can be written as Equation 5, except P_e is defined as the inelastic buckling strength. Hence, $P_n = F_{cr}A_g$, defined by the AISC column curve with no $0.8\tau_b$ stiffness reduction on E; $P_e = \pi^2(0.8\tau_b E)I/L^2$, which amplifies the moment; and $M_n = F_y Z$. The $0.8\tau_b$ stiffness reduction is not used in computing F_{cr} because the AISC column curve already has a stiffness reduction included. According to the AISC *Specification* (2016b) and given that all sections are compact, τ_b is calculated as:

$$\tau_b = 4\left(\frac{P}{P_y}\right)\left[1 - \left(\frac{P}{P_y}\right)\right] \text{ for } \frac{P}{P_y} > 0.5 \tag{6a}$$

$$\tau_b = 1 \text{ for } \frac{P}{P_y} \le 0.5 \tag{6b}$$

where $P_y = F_y A_g$.

Design by Advanced Elastic Analysis Method (DMMI)

As described earlier, DMMI is an alternative design method that may be particularly useful for more complex structures in which the unbraced length is not discernible. By directly modeling member out-of-straightness and representing potential inelasticity through the use of the stiffness reduction strategy employed in DM, the nominal axial strength, P_n, of the member may be taken as its cross-section strength. The resulting increase in axial strength, P_n, that appears in the interaction equation is compensated for by a larger required flexural strength, M_u, which is obtained from an advanced elastic structural analysis that accounts for initial system and member imperfections, second-order (geometric nonlinear) effects, and stiffness reduction due to inelasticity.

In contrast to the preceding analysis for determining strengths for ELM and DM, the analysis for DMMI must also include the direct modeling of member out-of-straightness. In this study, the shape of the initial imperfection is assumed a sine wave with an amplitude at midspan of $\delta_0 = L/1000$ per the AISC *Code of Standard Practice for Steel*

Buildings and Bridges (AISC, 2016a). As such, the second-order P-δ effect needs to include both the impact of the applied axial force and bending moment as well as the initial imperfection.

The solution to the governing differential equation, Equation 3, has a solution at midspan that is given by:

$$v\left(\frac{L}{2}\right)=\frac{\delta_0}{1-\frac{P}{P_e}}+\frac{M}{P}\left[\frac{2\sin\left(\sqrt{\frac{P}{P_e}}\frac{\pi}{2}\right)-\sin\left(\sqrt{\frac{P}{P_e}}\pi\right)}{\sin\left(\sqrt{\frac{P}{P_e}}\pi\right)}\right] \tag{7}$$

With $v(L/2)$, equilibrium on the deformed shape at midspan will result in a required moment strength of:

$$\left|M_{u_{mid}}\right|=M+Pv\left(\frac{L}{2}\right) \tag{8}$$

This solution is more complex than Equation 4 because the initial imperfection is not zero and contributes to the second-order effects.

Similar to DM, a stiffness reduction factor of $0.8\tau_b$ should be applied to all the members of the system, which in this study means that all EI terms (within P_e) in the previous equations should be $0.8\tau_b EI$. With values of $P_u = P$ and $M_u = \left|M_{u_{mid}}\right|$ as defined previously, the interaction equation (Equation 1a) is expressed for DMMI as:

$$\frac{P}{\phi P_n}+\frac{8}{9}\left[\frac{M+Pv\left(\frac{L}{2}\right)}{\phi M_n}\right]\leq 1.0 \tag{9}$$

in which, specific to DMMI, $v(L/2)$ is determined by Equation 7 with $\delta_0 = L/1000$ and P_e and τ_b as defined for DM, $P_n = F_y A_g$, and $M_n = F_y Z$.

Design by Advanced Inelastic Analysis Method (GMNIA)

Since 2010, the design by advanced inelastic analysis method has been provided in AISC *Specification* Appendix 1. Given that this design method is based on a geometric and materially nonlinear analysis that includes initial imperfections, it will be referenced by the acronym GMNIA. The second-order inelastic analysis routines used in this study are included in the finite element analysis software FE++ (Alemdar, 2001) for W-shapes and STRAND7 for HSS, where distributed plasticity models are employed. In FE++, each beam-column is modeled by eight line elements, thereby permitting a sine wave member out-of-straightness of $\delta_0 = L/1000$ to be directly modeled in the analysis. Residual stresses are represented by pre-stressing (compression or tension) the fibers that define the cross section. In STRAND7, however, shell elements are used to model the beam-columns, and similarly for FE++, member out-of-straightness and residual stresses are directly modeled. In both analysis programs, the applied axial force P and bending moments M are applied simultaneously, and an incremental-iterative arc-length solution scheme is employed until a limit point is achieved. Because of the relatively high accuracy of these analyses, the following error analyses of the preceding elastic design methods are based on the combinations of P and M that this inelastic design method would permit and still satisfy the provisions of AISC *Specification* Appendix 1.

It is well known that partial yielding of the cross section can have a significant effect on the stability of beam-columns. In cases where member out-of-straightness is not removed by processes, such as rotary straightening, this partial yielding can be accentuated by the presence of residual stresses. On the other hand, the use of such straightening processes can be shown to alleviate or even eliminate the presence of residual stresses (Ge and Yura, 2019). As a result, ultimate strength combinations were determined for cases in which residual stresses are and are not included in the analysis of elastic-perfectly plastic material models. When residual stresses are taken into account, the Galambos and Ketter (1959) residual stress distribution was employed for the W-shapes with a maximum compressive stress at the flange tips of $0.3F_y$. For the HSS-shapes, two residual stress patterns were considered. The Mathur (2011) residual stress pattern was employed to represent the highest expected residual stress pattern, with a maximum compressive strength of 20 ksi at the center of each face. A much lower and perhaps more realistic European Convention for Constructional Steelwork (ECCS, 1984) residual stress pattern with $0.2F_y$ at the center of each face was also studied. It is noted that the use of the Mathur pattern is considered conservative because it was developed for welded box columns. Additionally, the material elastic modulus, E, and yield stress, F_y, in the FE++ and STRAND7 analyses are reduced by a factor of 0.90, as required by AISC *Specification* Appendix 1.

NORMALIZED *P-M* INTERACTION CURVE AND ERROR CALCULATIONS

To compare the accuracy of each of the design methods, with special attention on DMMI, normalized *P-M* interaction curves of ELM, DM, DMMI, and GMNIA are first plotted. Data points are obtained by determining the maximum combination of axial load P and bending moments M that can be applied at the member ends such that the strength requirements of the design method would just be satisfied—that is, interaction Equation 1 equals 1.0. Calculation of error values in the curves are then computed using the GMNIA curve as a basis. To further allow the errors to be comparable for the wide range of member slenderness ratios investigated, all axial forces and moments were normalized by the maximum GMNIA values, with P^{GMNIA} being the maximum axial strength when the applied moment is $M = 0$ and with M^{GMNIA} being the maximum moment strength when the applied axial force is $P = 0$ (which would equal $0.9F_yZ$ for all members in this study). As an example, Figure 2 shows the normalized *P-M* interaction curves and a plot of the radial errors for a W12×120 member with an $L/r = 90$ that is subjected to minor-axis bending and with residual stresses included. Similar results for other L/r ratios for this W12×120 are provided in Appendix 1.

Using radial lines at 10° increments measured clockwise from the normalized *P*-axis to the *M*-axis, the intersections of the radial lines and the *P-M* curves are determined. It is noted that values at intersection points that lay between computed data points are obtained from a parabolic interpolation between the adjacent three data points. The percent errors of the design methods are then established by comparing their radial *R*-distances from the origin to the interaction curves according to:

$$\text{Percent radial error} = \frac{R_{XXX} - R_{GMNIA}}{R_{GMNIA}} \times 100\% \qquad (10)$$

where R_{XXX} is the radial distance of the *P-M* curves for the elastic design methods (ELM, DM, and DMMI), and R_{GMNIA} is the radial distance to the GMNIA *P-M* curve. As a result, error plots at different radial angles, as shown in Figure 2(b), represent a comprehensive range of different combinations of applied axial force and moment. Points with positive percent errors are indicative of situations in which the elastic design method (ELM, DM, or DMMI) is unconservative when compared to a design strength determined by GMNIA.

The legend within the rightward radial error graph [Figure 2(b)] contains information important to this study. Working from the top downward, rows within this legend represent results for the ELM, DM, and DMMI methods, respectively. The first two numbers in each row represent the error of each design method with an angle, θ, that corresponds to where the DMMI error is at its maximum. The second two numbers correspond to the maximum error of each design method and the angle, θ, where this maximum occurs.

CROSS SECTIONS INVESTIGATED

As indicated in Table 1, this study investigated 65 wide-flange shapes of ASTM A992 steel (E = 29,000 ksi and F_y = 50 ksi) and 4 HSS-shapes of ASTM A500 steel (E = 29,000 ksi and F_y = 46 ksi). These shapes are all of the compact sections that appear in the column design portion of the AISC *Steel Construction Manual* (AISC, 2017), and, for the most part, the wide-flange shapes investigated have depth-to-width ratios less than 1.5.

RESULTS

Interaction curves and plots of percent radial errors that correspond to the four different design methods (ELM, DM, DMMI, and GMNIA) were prepared (see, e.g., Figure 2) for

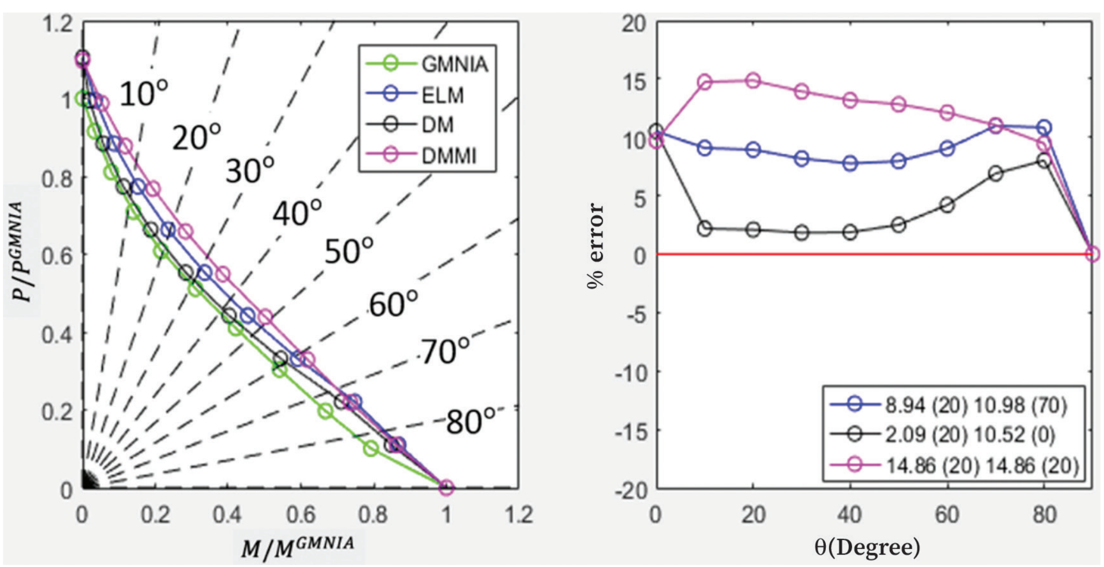

(a) Normalized P-M interaction curves for the four design methods

(b) Plots of percent radial errors

Fig. 2. For a W12×120 member with an L/r = 90 subject to minor-axis bending and with residual stresses included.

Table 1. Sections Studied							
W14	W14×730	W14×665	W14×605	W14×550	W14×500	W14×455	W14×426
	W14×398	W14×370	W14×342	W14×311	W14×282	W14×257	W14×233
	W14×211	W14×193	W14×176	W14×159	W14×145	W14×132	W14×120
	W14×109	W14×82	W14×74	W14×68	W14×61	W14×53	W14×48
W12	W12×336	W12×305	W12×279	W12×252	W12×230	W12×210	W12×190
	W12×170	W12×152	W12×136	W12×120	W12×106	W12×96	W12×87
	W12×79	W12×72	W12×58	W12×53	W12×50	W12×45	W12×40
W10	W10×112	W10×100	W10×88	W10×77	W10×68	W10×60	W10×54
	W10×49	W10×45	W10×39	W10×33			
W8	W8×67	W8×58	W8×48	W8×40	W8×35		
HSS	HSS12×12×½	HSS10×10×½	HSS8×8×½	HSS6×6×½			

all 65 W-shapes and 4 HSS-shapes over a range of member slenderness L/r ratios of 30, 60, 90, 120, and 150, with $r=\sqrt{I/A}$. With four cases, including minor- or major-axis bending for W-shapes and with or without residual stresses, this study evaluates 1,340 conditions, which are represented by a total of 58,960 analysis data points.

Wide-Flange Shapes

A summary of the results for all W-shapes is provided in Table 2, in which the maximum, average, and median of all of the individual member maximum percent radial errors are reported. In general, the percent radial errors reported for the three design methods are fairly similar. The largest percent radial errors are always for the DMMI method, and the smallest percent radial errors are for the DM method. Given that the ELM and DM methods are essentially the same, except that DM requires the analysis to include the stiffness reduction, $0.8\tau_b$, it is expected (and confirmed in Table 2) that DM will be more conservative (smaller radial errors) than ELM for all slenderness ratios. It is further noted that larger unconservative errors for DMMI for sections with residual stresses consistently occur when the applied loading combination is predominately axial force ($\theta = 10°$); in contrast, the larger unconservative errors for ELM and DM occur when the loading is primarily bending ($\theta = 80°$).

Hollow Structural Sections

The HSS-shape study does not include the parameter of bending axis because only square shapes are investigated. However, the effect of residual stress pattern is still investigated. A summary of the results for all HSS-sections is provided in Table 3. With the Mathur residual stress pattern, DMMI gives the largest percent radial errors among the three elastic design methods, a trend found consistent with W-shapes results. With the ECCS residual stress pattern, however, ELM gives the largest errors, while the errors of DMMI and DM are fairly close. It is worth noting that because the HSS shapes are modeled as square tubes without the curved corner geometry in STRAND7, the radius of gyration r of the STRAND7 model is slightly different from the AISC value, and consequently, the slenderness ratio L/r of HSS sections studied are close, but not exactly equal to 30, 60, 90, 120, and 150.

DISCUSSION

As would be expected, not including a residual stress distribution increases the design capacities of the beam-columns per the GMNIA design method. As a consequence, and given that the GMNIA results form the basis for the error analysis, the unconservative percent radial errors for all three of the elastic design methods (ELM, DM, and DMMI) are significantly reduced. A representative example of this is shown in Figure 3, where the performance of the DMMI design method is significantly improved with much better agreement (smaller radial errors) with GMNIA.

This increase in accuracy, however, is relatively pronounced where θ is small, which is a condition when the axial load is more significant than the bending moment, and is less obvious when θ is large, which is a combination of a larger bending moment and a smaller axial force. Of course, this is expected because it is well known that such residual stresses rarely affect the strength of a member subjected to a loading combination that is predominately bending (again noting that all members in this study are either subject to minor-axis bending or laterally braced when subject to major-axis flexure). The trend observed in Figure 3 is consistent for all shapes and design methods investigated in this study, regardless of the cross-sectional shapes, slenderness ratio, or the axis of bending investigated. In general,

Table 2. Summary of Percent Radial Errors of W-Shapes Studied for Minor- and Major-Axis Bending with and without Residual Stresses Included in the GMNIA Design					
		Minor-Axis, Residual Stresses	**Minor-Axis, No Residual Stresses**	**Major-Axis, Residual Stresses**	**Major-Axis, No Residual Stresses**
$L/r = 30$	DMMI	Max = 3.0% Ave = 2.2% Median = 2.2%	Max = 1.8% Ave = 0.5% Median = 0.4%	Max = 7.0% Ave = 6.5% Median = 6.6%	Max = 5.9% Ave = 5.0% Median = 5.0%
	ELM	Max = 3.2% Ave = 2.1% Median = 2.0%	Max= 2.5% Ave= 1.1% Median= 1.1%	Max = 6.9% Ave = 6.1% Median = 6.2%	Max = 5.8% Ave = 4.7% Median = 4.6%
	DM	Max = 2.6% Ave = 1.5% Median = 1.5%	Max = 1.9% Ave = 0.6% Median = 0.5%	Max = 6.0% Ave = 5.1% Median = 5.2%	Max = 4.9% Ave = 3.8% Median = 3.6%
$L/r = 60$	DMMI	Max = 14.8% Ave = 13.7% Median = 13.9%	Max = 7.3% Ave = 6.1% Median = 6.1%	Max = 10.5% Ave = 10.0% Median = 10.0%	Max = 7.5% Ave = 6.7% Median = 6.6%
	ELM	Max = 9.7% Ave = 8.4% Median = 8.4%	Max = 8.8% Ave = 7.5% Median = 7.6%	Max = 9.2% Ave = 8.5% Median = 8.6%	Max = 6.1% Ave = 5.2% Median = 5.3%
	DM	Max = 8.2% Ave = 7.3% Median = 7.3%	Max = 6.7% Ave = 5.5% Median = 5.5%	Max = 6.4% Ave = 5.7% Median = 5.8%	Max = 3.6% Ave = 2.9% Median = 3.0%
$L/r = 90$	DMMI	Max = 15.8% Ave = 14.8% Median = 14.8%	Max = 9.7% Ave = 8.2% Median = 8.2%	Max = 10.0% Ave = 9.2% Median = 9.2%	Max = 5.4% Ave = 4.7% Median = 4.7%
	ELM	Max = 13.0% Ave = 11.1% Median = 11.1%	Max = 11.3% Ave = 9.8% Median = 9.8%	Max = 7.6% Ave = 6.9% Median = 6.9%	Max = 4.5% Ave = 3.5% Median = 3.5%
	DM	Max = 11.2% Ave = 9.6% Median = 9.6%	Max = 8.2% Ave = 6.7% Median = 6.7%	Max = 3.9% Ave = 3.2% Median = 3.3%	Max = 1.5% Ave = 0.6% Median = 0.6%
$L/r = 120$	DMMI	Max = 15.3 % Ave = 14.2% Median = 14.1%	Max = 11.0% Ave = 9.6% Median = 9.6%	Max = 7.1% Ave =6.2% Median = 6.2%	Max = 2.9% Ave = 2.2% Median = 2.2%
	ELM	Max = 12.7% Ave = 11.3% Median = 11.3%	Max = 11.4% Ave = 9.9% Median = 9.9%	Max = 5.8% Ave = 4.6% Median = 4.6%	Max = 2.7% Ave = 1.8% Median = 1.8%
	DM*	Max = 9.5% Ave = 8.0% Median = 8.0%	Max = 8.1% Ave = 6.6% Median = 6.6%	Max = 2.6% Ave = 1.5% Median = 1.4%	Max = n/a* Ave = n/a Median = n/a
$L/r = 150$	DMMI	Max = 14.0% Ave = 12.6% Median = 12.6%	Max = 11.8% Ave = 10.4% Median = 10.4%	Max = 5.6% Ave = 4.8% Median = 4.7%	Max = 2.1% Ave = 1.2% Median = 1.2%
	ELM	Max = 12.4% Ave = 10.9% Median = 10.9%	Max = 11.2% Ave = 9.8% Median = 9.8%	Max = 4.4% Ave = 3.4% Median = 3.4%	Max = 1.4% Ave = 0.5% Median = 0.5%
	DM*	Max = 9.0% Ave = 7.6% Median = 7.6%	Max = 7.8% Ave = 6.4% Median = 6.4%	Max = 1.1% Ave = 0.2% Median = 0.1%	Max = n/a Ave = n/a Median = n/a
Note: No unconservative errors are observed as indicated by n/a					

Table 3. Summary of Percent Radial Errors of HSS Sections Studied with High and Low Residual Stresses Included in the GMNIA Design			
		High Residual Stress (Mathur)	**Low Residual Stress (ECCS)**
$L/r = 30$	DMMI	Max = 1.7% Ave = 1.4% Median = 1.4%	Max = 1.3% Ave = 0.7% Median = 1.0%
	ELM	Max = 1.6% Ave = 1.1% Median = 1.1%	Max = 1.3% Ave = 0.8% Median = 1.0%
	DM	Max = 1.6% Ave = 1.1% Median = 1.1%	Max = 1.3% Ave = 0.7% Median = 1.0%
$L/r = 60$	DMMI	Max = 10.0% Ave = 9.6% Median = 9.5%	Max = 2.4% Ave = 1.6% Median = 1.8%
	ELM	Max = 5.4% Ave = 4.3% Median = 4.1%	Max = 3.1% Ave = 2.6% Median = 2.4%
	DM	Max = 3.8% Ave = 3.3% Median = 3.3%	Max = 2.4% Ave = 1.6% Median = 1.8%
$L/r = 90$	DMMI	Max = 17.5% Ave = 16.2% Median = 16.2%	Max = 3.5% Ave = 2.9% Median = 2.9%
	ELM	Max = 14.6% Ave = 13.2% Median = 13.1%	Max = 4.8% Ave = 4.3% Median = 4.1%
	DM	Max = 14.6% Ave = 13.2% Median = 13.1%	Max = 3.5% Ave = 2.9% Median = 2.9%
$L/r = 120$	DMMI	Max = 14.8% Ave = 14.1% Median = 14.3%	Max = 5.7% Ave = 3.7% Median = 3.5%
	ELM	Max = 13.6% Ave = 11.8% Median = 11.8%	Max = 5.7% Ave = 5.2% Median = 5.1%
	DM	Max = 13.6% Ave = 11.6% Median = 11.8%	Max = 5.7% Ave = 3.7% Median = 3.5%
$L/r = 150$	DMMI	Max = 17.0% Ave = 15.9% Median = 15.7%	Max = 6.3% Ave = 4.0% Median = 4.1%
	ELM	Max = 11.7% Ave = 11.4% Median = 11.4%	Max = 5.7% Ave = 5.6% Median = 5.7%
	DM	Max = 8.3% Ave = 8.0% Median = 8.0%	Max = 5.7% Ave = 4.0% Median = 4.1%

the reduction in DMMI errors for sections without residual stresses is largest for W-shapes when the slenderness ratio is L/r = 60 for minor-axis bending and L/r = 90 for major-axis bending. In moving from high to low residual stresses, the reduction is largest when slenderness ratio of HSS-sections is L/r = 90. The change in error is the smallest at the extreme slenderness ratios investigated, including the least-slender (L/r = 30) and most-slender (L/r = 150) members for W-shapes, and when the beam-column is stocky (L/r = 30) for HSS-sections. It is further noted that the ELM and DM design methods can be significantly more conservative when residual stresses are not present.

From the W-shape results in this study, it can be observed that with the exception of more-stocky members (L/r = 30), the percent radial errors for all three design methods, especially DMMI, are reduced when members are subject to major-axis bending instead of minor-axis bending.

As further shown in Tables 2 and 3, all three elastic design methods will produce some unconservative errors when compared with GMNIA-based design in most of the cases studied. For the reasons given earlier, DM will always provide smaller percent radial errors when compared with ELM. It is important to note that this applies only for the simply supported member explored in this study—for systems comprised of members with effective length K-factors exceeding 1.0, this will not necessarily be the case (Martinez-Garcia and Ziemian, 2006).

The results for DMMI and ELM are not significantly different, with the largest differences occurring for W-shape members subject to minor-axis bending in the low- to mid-slenderness (L/r = 60 to 90), and for HSS-section member with L/r = 60.

SUMMARY AND CONCLUSION

This study evaluates three elastic design methods (ELM, DM, and DMMI) appearing in the 2016 AISC *Specification* by making comparisons with a fourth method (GMNIA) that is often considered the most "exact" because all destabilizing effects are explicitly modeled in the analysis. This latter method, design by advanced inelastic analysis, also appears in the AISC *Specification*. With 1,340 conditions studied that required a total of 58,960 analyses, simply supported beam-columns comprised of a fairly wide range of column W- and HSS- sections and slenderness ratios are investigated for conditions of minor- or major-axis flexure that include or exclude the presence of residual stresses. In all cases, members are assumed to be fully braced out-of-plane.

In general, all three elastic design methods provide fairly similar results. AISC's relatively new design by advanced elastic analysis method, termed DMMI in this

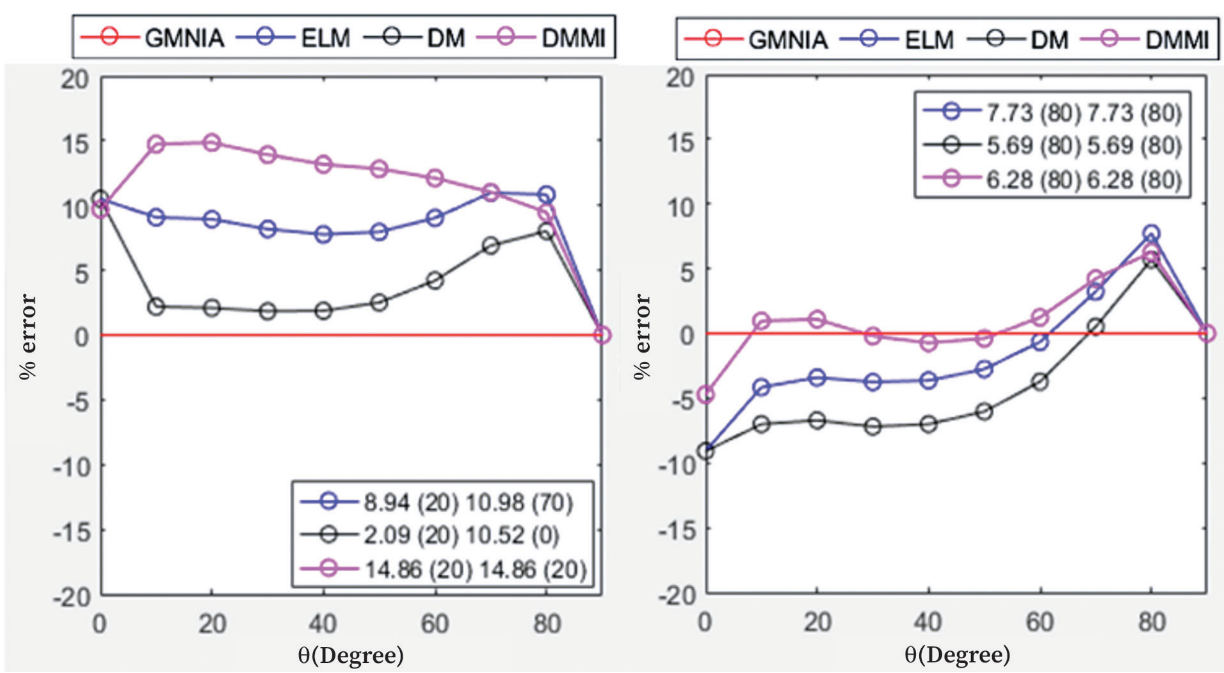

(a) Residual stresses included in the GMNIA-based design

(b) Residual stresses excluded in the GMNIA-based design

Fig. 3. Percent radial errors for a member of an L/r = 60 *subjected to minor-axis bending comprised of a* W12×120 *section.*

study, consistently indicated more strength (1% to 5%) than AISC's effective length method. Conditions of major-axis bending for W-shapes significantly improved the performance of all three elastic design methods. Regardless of the axis of bending, results are always improved when residual stresses are lowered or eliminated, a condition that is quite common for HSS-shapes and often the consequence of rotary straightening W-shapes during the rolling process. Knowing that ELM has been an established design method that has performed well in the United States since the early 1960s, it is the authors' opinion that the unconservative errors for all three elastic design methods may not be reason for significant concern. Based on the many systems previously investigated by the second author in the development of AISC's design by advanced elastic analysis method (DMMI), the study presented in this paper has provided some well-served deserved investigations on beam-columns subject to minor-axis bending.

Noting that AISC's design by advanced elastic analysis method currently only permits that the axial strength P_n can be taken as the cross-section strength P_y, additional studies are needed to permit this approach to move to a full cross-section-based design method—in other words, move from requiring the flexural strength M_n to account for member length effects, such as lateral-torsional buckling, to being taken as cross-section strength M_p. Of course, such a revision will require that engineers have access to commercially available analysis software that directly models nonuniform torsion, and thereby permits the analysis to account for the rapid increase in moments as lateral-torsional and flexural-torsional buckling modes of failure are approached.

ACKNOWLEDGEMENTS

The authors gratefully acknowledge Gigi Rojahn for providing the STRAND7 data, which provided the HSS-section GMNIA results as a basis for comparison.

APPENDIX A

Plots of Interaction Curves and Percent Radial Error

As a complement to Figure 2, the remaining normalized *P-M* interaction curves and corresponding plots of percent radial errors that were studied for the specific case of a W12×120 member that includes residual stresses and subjected to minor-axis bending are provided in Figures A-1 through A-4.

APPENDIX B

Data for Plots of Percent Radial Errors

Tables B-1 through B-5 provide numerical values for the data points appearing in the percent radial error plots given in Figure 2 and Appendix A, and for similar plots for the presented example of a W12×120. These percent radial errors represent the minor- and major-axis bending cases for when residual stresses are either included or excluded. A positive error value indicates nonconservative error when compared to GMNIA results, and likewise, a negative error represents conservative error.

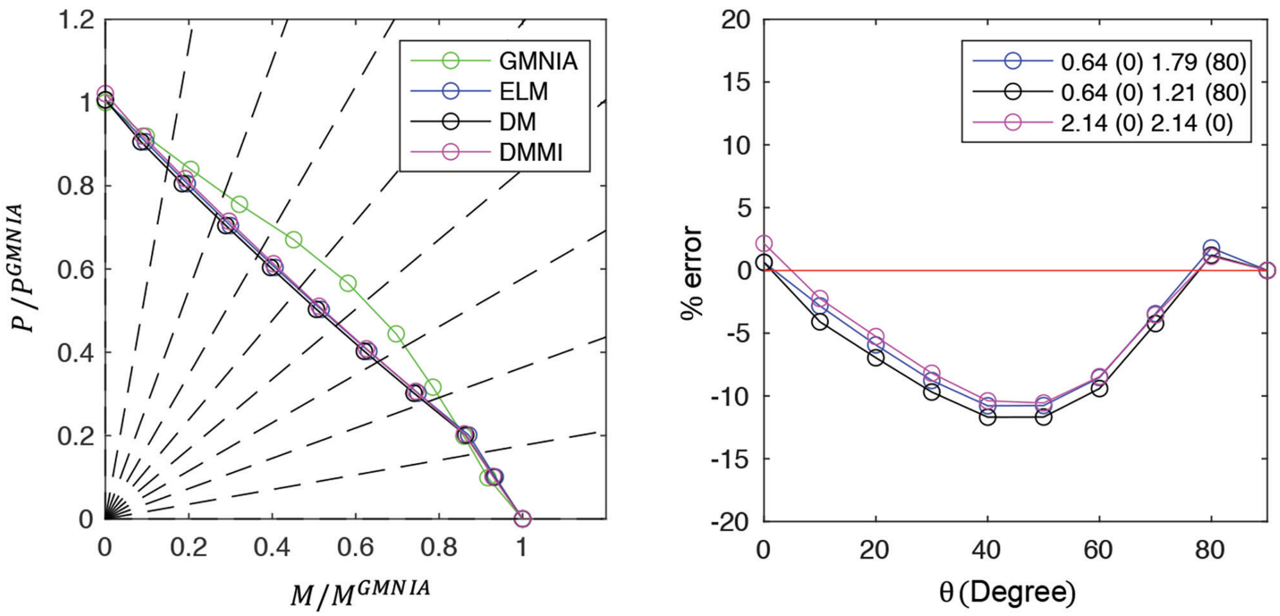

Fig. A-1. L/r = *30.*

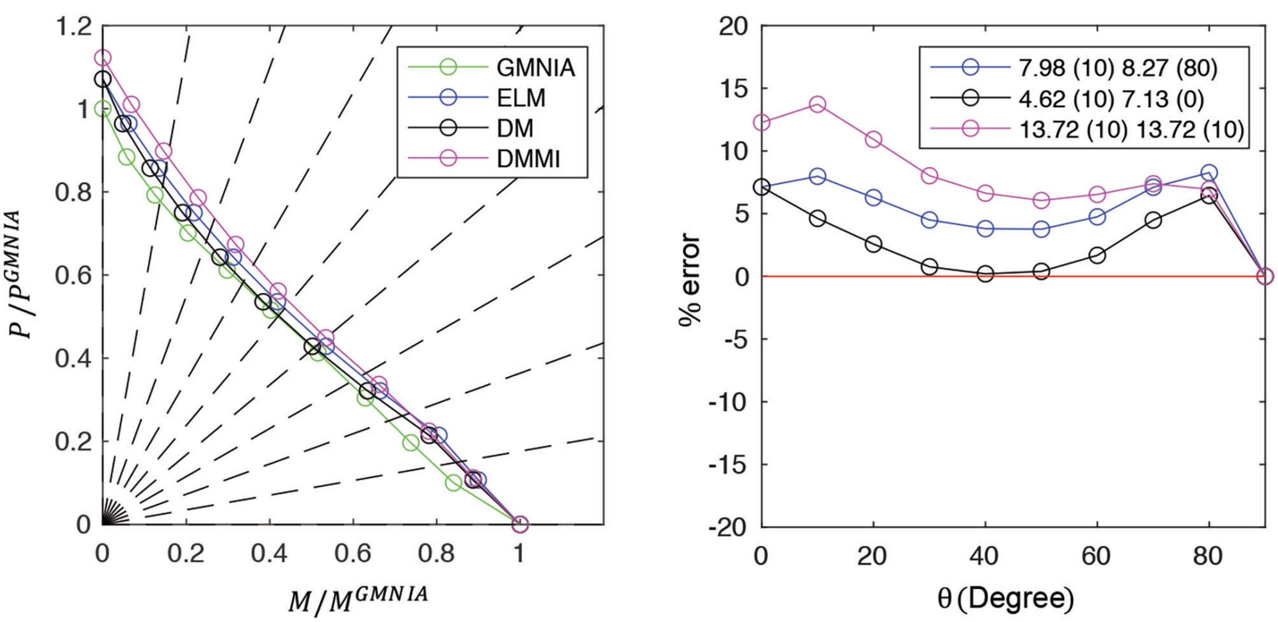

Fig. A-2. L/r = *60.*

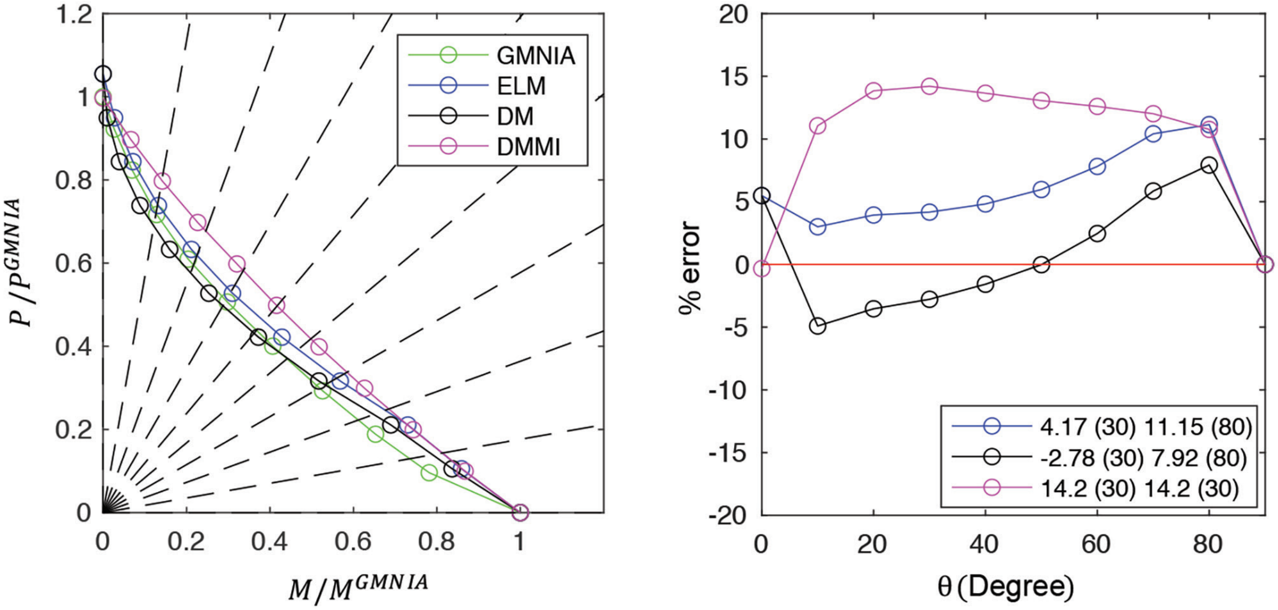

Fig. A-3. L/r = *120.*

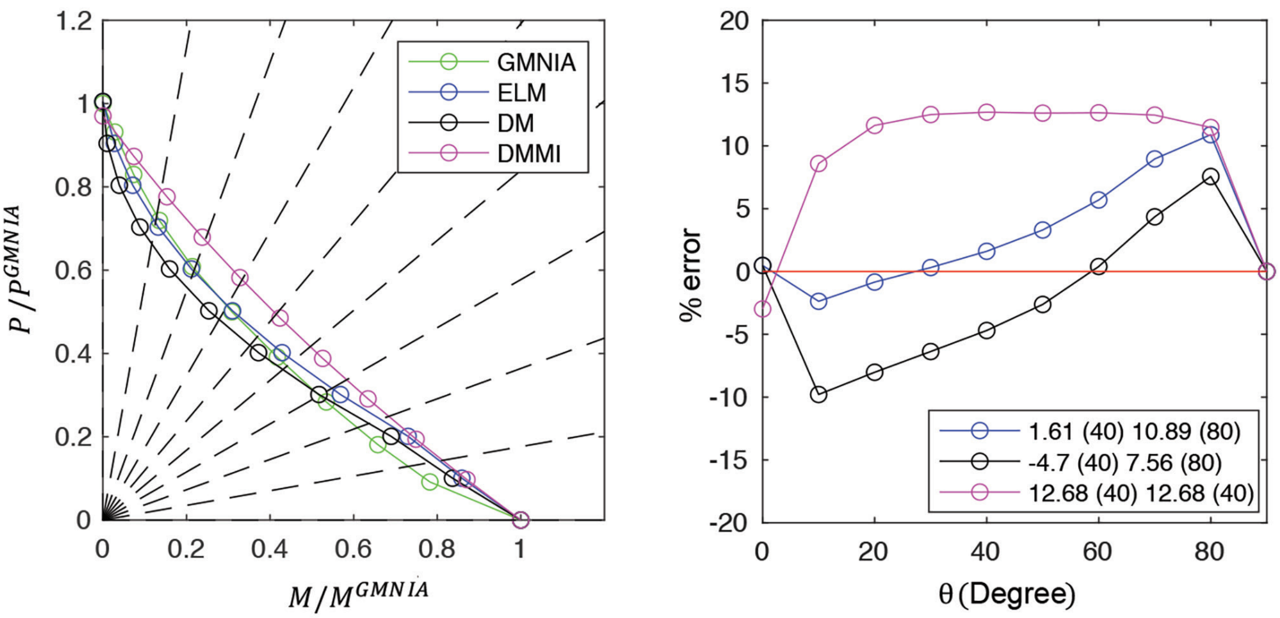

Fig. A-4. L/r = *150.*

Table B-1. $L/r = 30$ (values are percent radial errors)												
	Minor-Axis Bending with Residual Stresses			Minor-Axis Bending without Residual Stresses			Major-Axis Bending with Residual Stresses			Major-Axis Bending without Residual Stresses		
θ	DMMI	ELM	DM	DMMI	ELM	DM	DMMI	ELM	DM	DMMI	ELM	DM
0°	2.1	0.6	0.6	–6.0	–7.4	–7.4	2.1	–0.2	–0.2	–0.8	–3.1	–3.1
10°	–2.2	–2.8	–4.1	–6.7	–7.2	–8.4	3.8	2.6	1.3	–0.2	–1.4	–2.6
20°	–5.3	–5.9	–7.0	–6.9	–7.6	–8.6	5.1	3.8	2.7	2.4	1.2	0.1
30°	–8.2	–8.8	–9.7	–9.6	–10.2	–11.1	5.8	4.6	3.6	3.2	2.1	1.1
40°	–10.4	–10.8	–11.7	–12.1	–12.5	–13.4	6.2	5.4	4.3	3.7	2.9	1.8
50°	–10.6	–10.8	–11.7	–12.9	–13.2	–14.1	6.5	5.9	4.8	4.5	3.9	2.9
60°	–8.5	–8.5	–9.4	–11.1	–11.2	–12.1	6.3	6.0	5.0	5.0	4.6	3.6
70°	–3.5	–3.4	–4.2	–6.0	–5.9	–6.7	5.9	5.8	5.0	4.6	4.5	3.6
80°	1.1	1.8	1.2	0.4	1.1	0.4	2.9	3.4	2.8	2.2	2.8	2.2
90°	0	0.0	0.0	0.0	0.0	0.0	0.0	0.0	0.0	0.0	0.0	0.0

Table B-2. $L/r = 60$ (values are percent radial errors)												
	Minor-Axis Bending with Residual Stresses			Minor-Axis Bending without Residual Stresses			Major-Axis Bending with Residual Stresses			Major-Axis Bending without Residual Stresses		
θ	DMMI	ELM	DM	DMMI	ELM	DM	DMMI	ELM	DM	DMMI	ELM	DM
0°	12.3	7.1	7.1	–4.7	–9.1	–9.1	3.8	–2.6	–2.6	–6.6	–12.4	–12.4
10°	13.7	8.0	4.6	1.0	–4.2	–7.0	6.8	0.3	–2.7	0.4	–5.8	–8.5
20°	10.9	6.3	2.6	1.1	–3.4	–6.7	8.1	2.5	–1.0	–0.3	–5.6	–8.8
30°	8.0	4.5	0.8	–0.2	–3.8	–7.2	8.5	4.0	0.3	3.1	–1.3	–4.9
40°	6.6	3.8	0.2	–0.7	–3.6	–7.0	9.0	5.3	1.6	4.8	1.0	–2.5
50°	6.1	3.8	0.4	–0.4	–2.8	–6.0	9.8	6.8	3.3	5.2	2.2	–1.3
60°	6.5	4.7	1.7	1.2	–0.7	–3.7	10.5	8.1	4.9	6.3	3.8	0.6
70°	7.4	7.1	4.5	4.2	3.2	0.5	9.5	8.5	5.7	7.0	5.5	2.7
80°	6.9	8.3	6.4	6.3	7.7	5.7	5.1	6.3	4.3	3.7	4.9	2.9
90°	0	0.0	0.0	0.0	0.0	0.0	0.0	0.0	0.0	0.0	0.0	0.0

Table B-3. $L/r = 90$ (values are percent radial errors)												
	Minor-Axis Bending with Residual Stresses			Minor-Axis Bending without Residual Stresses			Major-Axis Bending with Residual Stresses			Major-Axis Bending without Residual Stresses		
θ	DMMI	ELM	DM	DMMI	ELM	DM	DMMI	ELM	DM	DMMI	ELM	DM
0°	9.7	10.5	10.5	–2.7	–2.0	–2.0	0.4	–1.0	–1.0	–5.7	–7.0	–7.0
10°	14.7	9.1	2.2	2.2	–2.8	–8.8	4.1	–2.1	–8.1	–0.6	–6.5	–12.3
20°	14.9	8.9	2.1	3.3	–2.1	–8.2	5.4	–0.9	–7.1	0.3	–5.8	–11.6
30°	13.9	8.2	1.8	3.7	–1.7	–7.4	6.6	0.5	–5.4	2.4	–3.6	–9.4
40°	13.2	7.8	1.9	4.2	–0.9	–6.5	8.0	2.1	–3.6	3.9	–1.8	–7.5
50°	12.8	8.0	2.5	5.1	0.4	–4.8	9.2	3.9	–1.5	4.3	–0.9	–6.1
60°	12.1	9.0	4.2	6.5	2.9	–1.8	9.4	5.4	0.5	4.8	0.7	–4.1
70°	11.0	11.0	6.9	7.6	6.7	2.5	8.0	6.9	2.7	4.4	2.8	–1.3
80°	9.5	10.8	8.0	8.2	9.7	6.7	4.8	6.1	3.2	2.2	3.5	0.6
90°	0	0.0	0.0	0.0	0.0	0.0	0.0	0.0	0.0	0.0	0.0	0.0

Table B-4. $L/r = 120$ (values are percent radial errors)												
	Minor-Axis Bending with Residual Stresses			Minor-Axis Bending without Residual Stresses			Major-Axis Bending with Residual Stresses			Major-Axis Bending without Residual Stresses		
θ	DMMI	ELM	DM	DMMI	ELM	DM	DMMI	ELM	DM	DMMI	ELM	DM
0°	–0.3	5.5	5.5	–5.6	–0.1	–0.1	–5.7	–1.4	–1.4	–7.1	–2.9	–2.9
10°	11.1	3.0	–4.9	0.9	–6.3	–13.4	1.0	–7.0	–14.0	–1.1	–9.0	–15.8
20°	13.8	3.9	–3.5	3.2	–5.7	–12.5	3.6	–6.0	–12.8	0.4	–8.8	–15.4
30°	14.2	4.2	–2.8	4.9	–4.5	–10.8	5.4	–4.6	–10.9	1.2	–8.4	–14.5
40°	13.7	4.8	–1.6	5.8	–2.7	–8.7	6.0	–3.0	–9.0	1.5	–7.2	–13.0
50°	13.1	6.0	0.0	6.7	–0.2	–5.9	6.3	–1.1	–6.8	2.3	–4.9	–10.4
60°	12.6	7.8	2.5	7.7	2.8	–2.4	6.2	0.9	–4.2	2.3	–2.9	–7.8
70°	12.0	10.4	5.9	8.7	6.8	2.3	5.6	3.4	–1.0	2.1	–0.2	–4.5
80°	10.8	11.1	7.9	9.4	9.8	6.5	4.2	4.4	1.2	1.6	1.9	–1.2
90°	0	0.0	0.0	0.0	0.0	0.0	0.0	0.0	0.0	0.0	0.0	0.0

Table B-5. $L/r = 150$ (values are percent radial errors)												
	Minor-Axis Bending with Residual Stresses			Minor-Axis Bending without Residual Stresses			Major-Axis Bending with Residual Stresses			Major-Axis Bending without Residual Stresses		
θ	DMMI	ELM	DM	DMMI	ELM	DM	DMMI	ELM	DM	DMMI	ELM	DM
0°	–3.0	0.5	0.5	–6.5	–3.2	–3.2	–7.4	–4.9	–4.9	–9.4	–7.0	–7.0
10°	8.6	–2.4	–9.8	–0.2	–10.2	–17.0	–0.8	–11.3	–18.0	–4.8	–14.9	–21.2
20°	11.6	–0.8	–8.0	2.4	–9.0	–15.6	1.6	–10.3	–16.8	–1.9	–13.3	–19.6
30°	12.5	0.3	–6.4	4.2	–7.2	–13.4	2.8	–8.9	–15.0	0.0	–11.4	–17.3
40°	12.7	1.6	–4.7	5.7	–4.8	–10.8	3.6	–7.1	–13.0	0.7	–9.8	–15.5
50°	12.6	3.3	–2.6	7.1	–2.0	–7.7	4.3	–4.9	–10.4	0.1	–8.8	–14.2
60°	12.6	5.7	0.4	8.5	1.5	–3.6	4.7	–2.4	–7.4	0.5	–6.4	–11.3
70°	12.5	9.0	4.4	9.7	6.0	1.5	4.7	0.8	–3.5	1.0	–2.9	–7.1
80°	11.5	10.9	7.6	10.2	9.6	6.2	3.9	3.3	0.1	1.3	0.7	–2.5
90°	0	0.0	0.0	0.0	0.0	0.0	0.0	0.0	0.0	0.0	0.0	0.0

REFERENCES

AISC (2005), *Specification for Structural Steel Buildings*, ANSI/AISC 360-05, American Institute of Steel Construction, Chicago, Ill.

AISC (2010), *Specification for Structural Steel Buildings*, ANSI/AISC 360-10, American Institute of Steel Construction, Chicago, Ill.

AISC (2016a), *Code of Standard Practice for Steel Buildings and Bridges*, ANSI/AISC 303-16, American Institute of Steel Construction, Chicago, Ill.

AISC (2016b), *Specification for Structural Steel Buildings*, ANSI/AISC 360-16, American Institute of Steel Construction, Chicago, Ill.

AISC (2017), *Steel Construction Manual*, 15th Ed., American Institute of Steel Construction, Chicago, Ill.

Alemdar, B.N. (2001), "Distributed Plasticity Analysis of Steel Building Structural Systems," PhD dissertation, Georgia Institute of Technology, Atlanta, Ga.

ECCS (1984), "Ultimate Limit State Calculation of Sway Frames with Rigid Joints," Publication No. 33, European Convention for Constructional Steelwork, Brussels, Belgium.

Galambos, T.V. and Ketter, R.L. (1959), "Columns under Combined Bending and Thrust," *Journal of the Engineering Mechanics Division*, ASCE, Vol. 85, No. EM2, pp. 135–152.

Ge, X. and Yura, J. (2019), "The Strength of Rotary-Straightened Steel Columns," *Proceedings of the Annual Stability Conference*, SSRC, St. Louis, Mo., pp. 425–442.

Giesen-Loo, E. (2016), "Design of Steel Structures by Advanced 2nd-Order Elastic Analysis—Background Studies," Honors Thesis, Bucknell University, Lewisburg, Pa.

Martinez-Garcia, J.M. and Ziemian, R.D. (2006), "Benchmark Studies to Compare Frame Stability Provisions," *Proceedings of the Annual Technical Session and Meeting*, SSRC, San Antonio, Texas, pp. 425–442.

Mathur, K. (2011), "Effects of Residual Stresses and Initial Imperfections on Earthquake Response of Steel Moment Frames," Master of Science Thesis, University of Illinois at Urbana-Champaign, Urbana, Ill.

McGuire, W., Gallagher, R., and Ziemian, R. (2000), *Matrix Structural Analysis*, John Wiley & Sons, Inc., New York, N.Y.

Nwe Nwe, M.T. (2014), "The Modified Direct Analysis Method: An Extension of the Direct Analysis Method," Honors Thesis, Bucknell University, Lewisburg, Pa.

Wang, Y. (2018), "Advanced Analysis of Beam-Columns Resisting Minor Axis Bending," Honors Thesis, Bucknell University, Lewisburg, Pa.

Wang, Y. and Ziemian, R.D. (2019), "Design by Advanced Elastic Analysis—An Investigation of Beam-Columns Resisting Minor-Axis Bending," *Proceedings of the Annual Stability Conference,* SSRC, St. Louis, Mo.

Ziemian, R.D. (ed.) (2010), *Guide to Stability Design Criteria for Metal Structures*, John Wiley & Sons, Inc., Hoboken, N.J.